Evidence for late Carboniferous episodic marine incursions in eastern Laurasia

Trevor B. Kelly, Grant D. Wach

Basin and Reservoir Laboratory, Department of Earth Sciences, Dalhousie University

Summary

Astronomical tides are a consistent and reliable phenomenon that are generated by the gravitational pull exerted on oceans, and to a lesser extent, lakes, by the sun and the moon. When tidal forces are channeled between islands or into bays and estuaries, they are known as tidal currents (Shukla and Shukla 2013). Astronomical tides are grouped into three categories: 1) diurnal (one episode of high water and low water daily); 2) semi-diurnal (two episodes of high water and low water daily); and 3) mixed (comparable to semi-diurnal, except they do not rise and fall at same levels). A single neap/spring/neap cycle is characterized as having 28 dominant current events within a semi-diurnal tidal system and 14 dominant events within a diurnal tidal system respectively (De Boer et al. 1989; Friedman and Chakraborty 2006).

Despite the structures that can form in sedimentary environments, only a few (e.g., tidal rhythmites, regularly occurring mud drapes, flaser/lenticular bedding, and directional bimodality) support the indication of paleotidal influences and have added value for the construction of tidal deposit depositional models (Shukla and Shukla 2013). According to Boersma and Terwindt (1981), paleotidal activity is best exemplified by tidal rhythmites, since they are never developed in continental or fluvial depositional environments. Boersma (1969) was the first to introduce the tidal rhythmite term, which was used to define the depositional unit corresponding to one tidal cycle. Later, Visser (1980) was able to make a direct relationship between successively occurring lateral tidal rhythmites and neap-spring tidal cyclicity.

The Joggins Fossil Cliffs site was granted UNESCO World Heritage status because of its unmatched preservation of terrestrial life in their environmental context during the Pennsylvanian 'Coal Age'. Despite 185 years of research, important questions persist regarding the paleoenvironment, including the extent of marine influence. This study examines tidal rhythmites in the late Carboniferous strata of the Joggins Formation. In this research, we observed cycles within parallel, thinly laminated, vertically accreted tidal rhythmites. The examples include: 1) sand and mud couplets deposited during flow and slack water stages, respectively, which correlate to ebb and flood tidal cycles; 2) a variation in sand and mud lamination thickness due to changes in sand and mud availability during neap-spring tidal cycles; 3) spring couplet thickness variations demonstrating the lunar cycles of low and high spring tides; and 4) the variation of rhythmite thicknesses reflecting tidal variations with longer cycles or sediment concentration fluctuations.

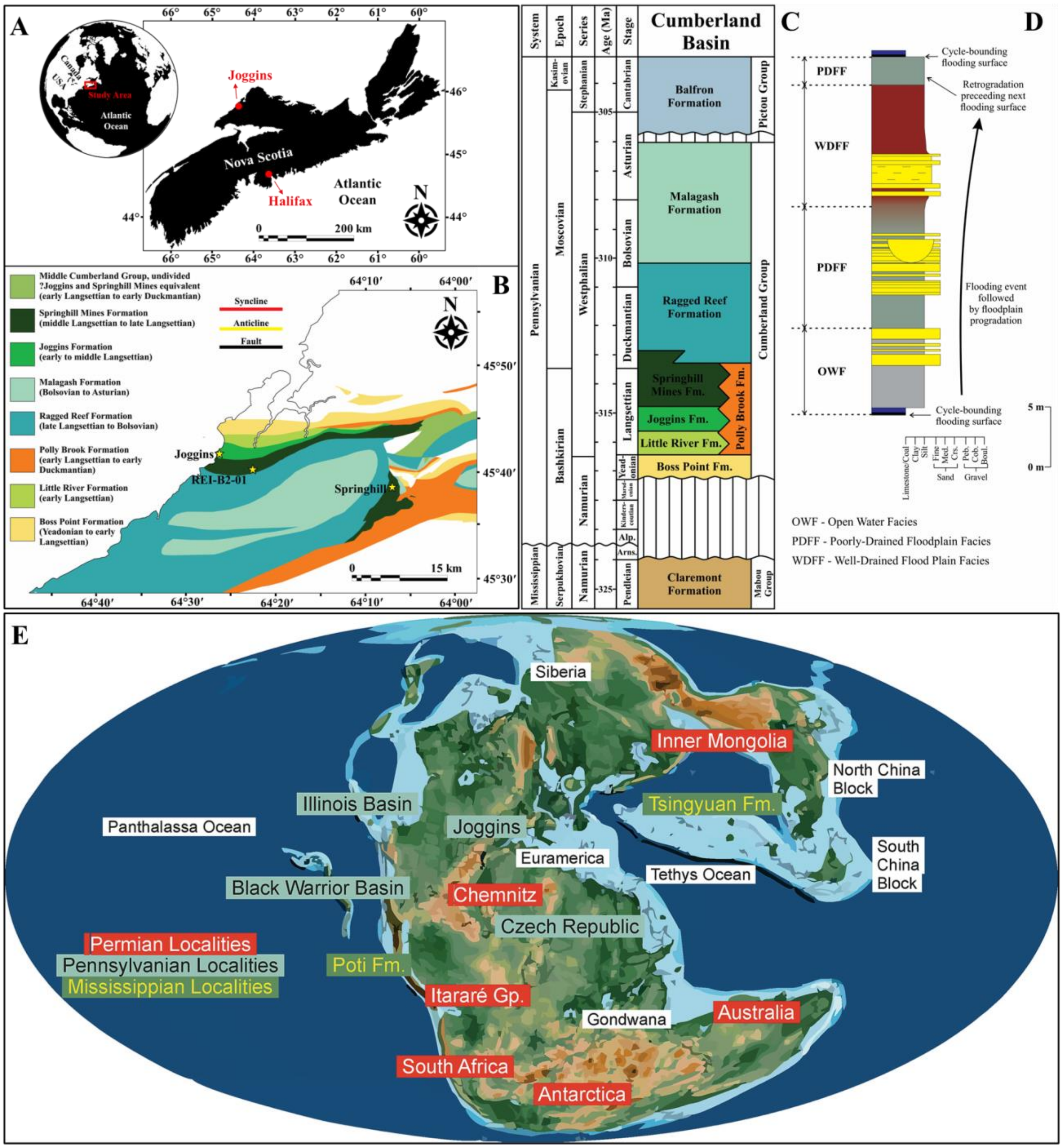

Figure 1. A) Location map showing the study area. B) A closeup view of the study area showing the Cumberland Group geological units and the location of the borehole in relation to Joggins and Springhill. C) The Cumberland Basin stratigraphic framework (modified from Gibling et al. 2008; Gibling et al. 2019). D) A representative measured section of the Joggins Formation (modified from Davies et al. 2005; Gibling et al. 2008; Gibling et al. 2019). E) Permian/Carboniferous paleogeographic map of Pangea showing the main physiographic provinces and the regions containing widespread coal deposits (Gastaldo et al. 2020).

Methods and Equipment

High resolution digital image acquisition. Digital images were acquired using a standard 12 mega-pixel (pixel resolution of 4,290 X 2,800) Samsung Galaxy S8+ paired with a home-built drill core photography apparatus. It was built solely for the purpose of acquiring high-resolution, constant height and width, panoramic photographs using the high-end camera present on modern smart phones.

High resolution digital drill core analysis. Digital images were imported into a vector graphics editor program where it was cropped. Using the dimensions of the core, the image was scaled to its true size. Measurements were recorded using the dimension measuring tool directly within the graphics program. The data that was collected allowed for the application of the Tessier and Gigot (1989) method to be used to synthesize the data from the core measurements, of successive tidal bundle thicknesses of mud and sand laminae.

Lamina-thickness and Fourier analysis. Lamina-thickness and Fourier analysis of rhythmites are extensively applied to test for and establish a tidal influence on sedimentation (Martino and Sanderson 1993; Hovikoski et al. 2005; O'Connell et al. 2017). The variable, alternating thicknesses of the tidal rhythmites is quantitatively exposed in a spectral analysis of the data. The application of the discrete Fourier transform function on the data in a Matlab script helps to elucidate the cycles and their amplitudes.

Results and Discussion

The core interval between ~ 810.71 m to ~ 811.02 m (Figure 2A) and ~ 1,003.40 m to ~ 1,003.60 m (Figure 2B) reveals alternating sand and mud laminations consistent with tidal rhythmites. The lamina-thickness plots show thicknesses of each sand and mud lamination.

The lamina-thickness plot for the interval between ~ 810.71 m and ~ 811.02 m is shown in Figure 3A. It represents data from a continuous succession of 516 successive laminae (Figure 2A). It reveals alternating sand- and mud-dominated rhythmites. The grey bars represent the thickness of sandstone and the black bars represent the thickness of mud drapes. The trend line (bold red line) is drawn with a moving average of 14 days. The resulting Fourier transformation of the same data is shown in Figure 3B.

The lamina-thickness plot for the interval between ~ 1,003.40 m and ~ 1,003.60 m is shown in Figure 3C. It represents data from a continuous succession of 79 successive laminae (Figure 2B). It reveals alternating sand- and mud-dominated rhythmites. The grey bars represent the thickness of sandstone and the black bars represent the thickness of mud drapes. The trend line (bold red line) is drawn with a moving average of 14 days. The resulting Fourier transformation of the same data is shown in Figure 3D.

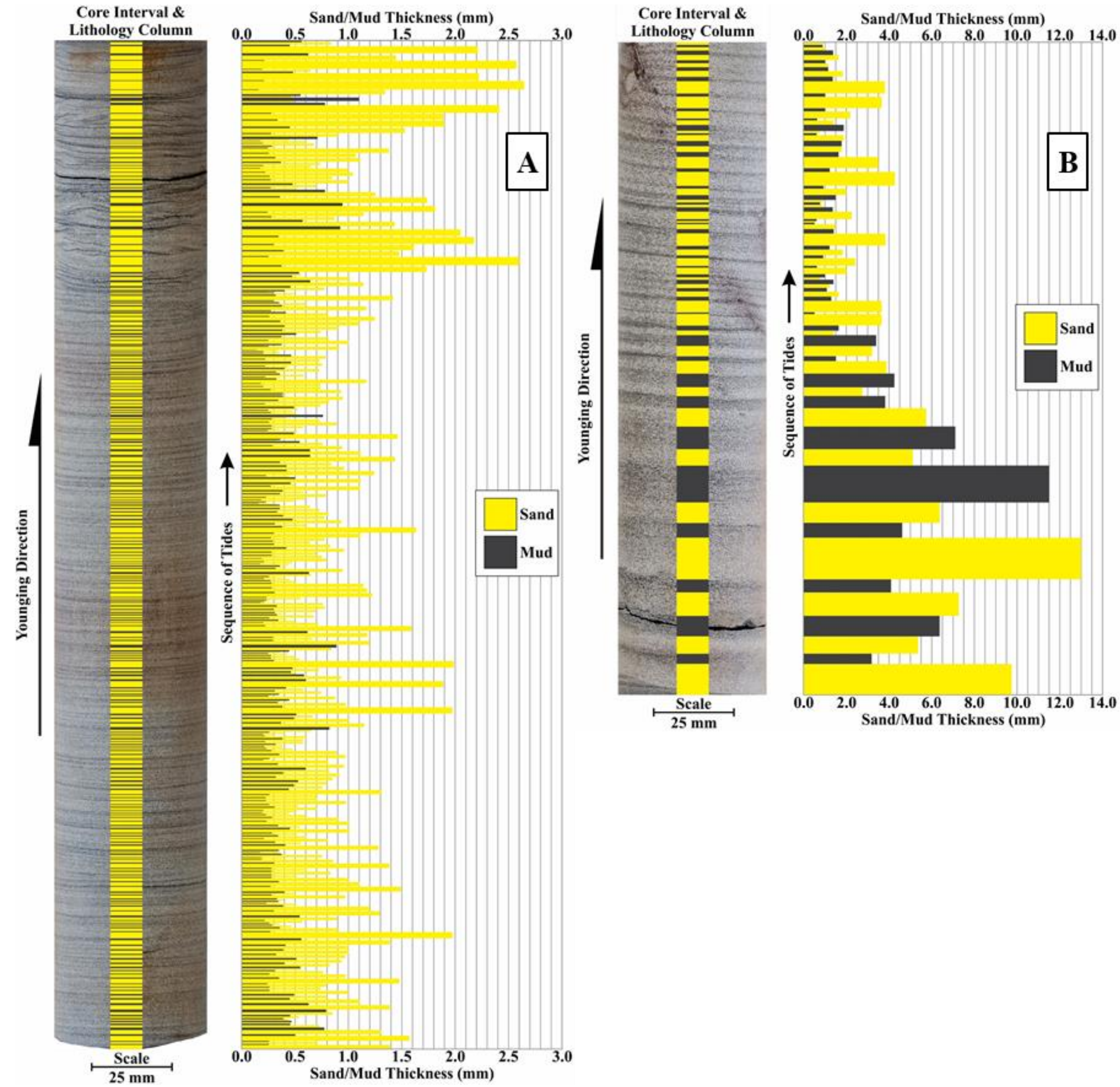

Figure 2. A) Digital photograph of core interval between ~ 810.71 m and ~ 811.02 m with a lithology column showing the sandstone/mudstone laminations. The lamina-thickness plot is to the right. B) Digital photograph of core interval between ~ 1,003.40 m and ~ 1,003.60 m with a lithology column showing the sandstone/mudstone laminations. The lamina-thickness plot is to the right.

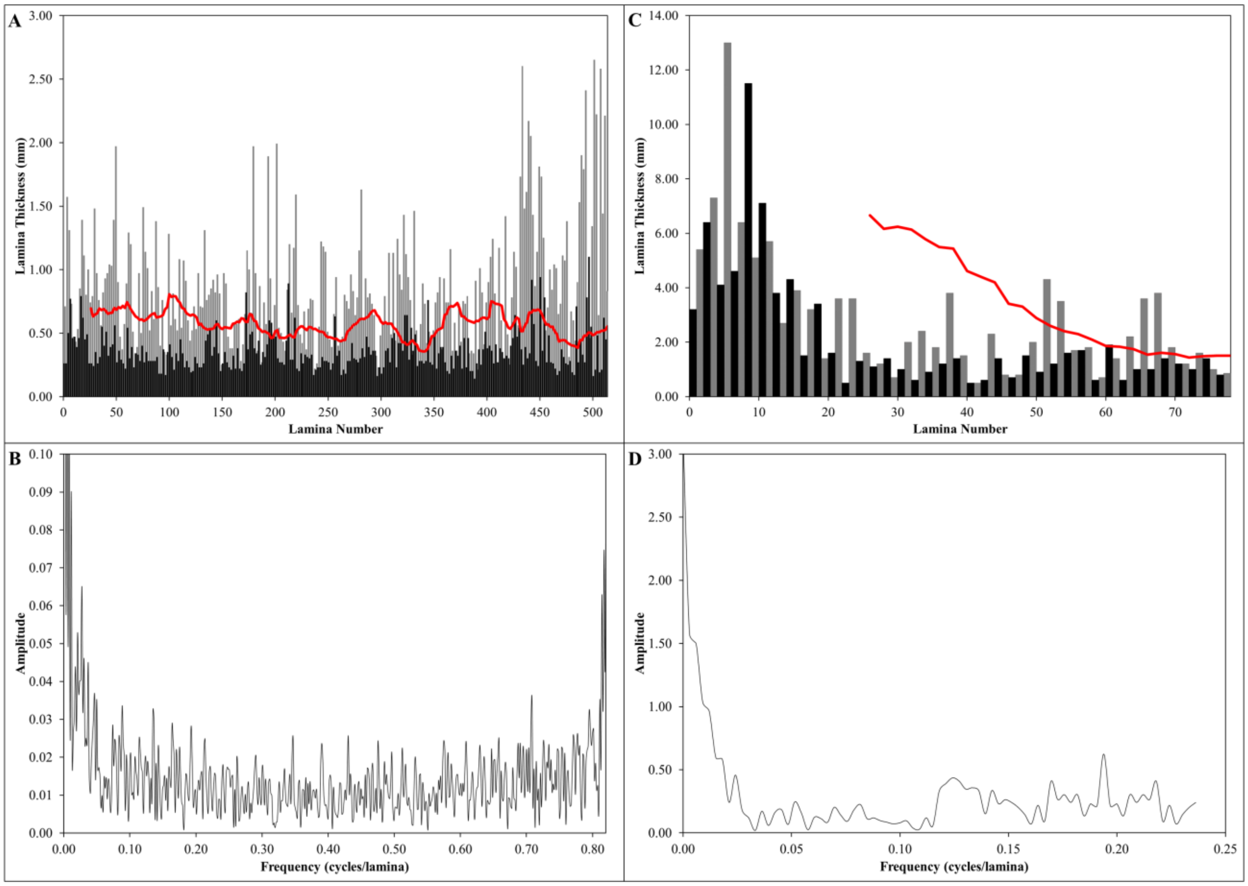

Figure 3. A) Lamina-thickness plot of 516 successive laminae from the interval between ~ 810.71 m and ~ 811.02 m. The grey bars represent the thickness of sandstone and the black bars represent the thickness of mud drapes. The trend line (bold red line) is drawn with a moving average of 14. The younging direction is from left to right. B) The resulting Fourier transformation of the same data. C) Lamina-thickness plot of 79 successive laminae from the interval between ~ 1,003.40 m and ~ 1,003.60 m. The grey bars represent the thickness of sandstone and the black bars represent the thickness of mud drapes. The trend line (bold red line) is drawn with a moving average of 14. The younging direction is from left to right. D) The resulting Fourier transformation of the same data.

Conclusions

This research provides evidence for episodic marine incursions during the late Carboniferous by way of successively accreting tidal rhythmites and a resulting neap-spring tidal cyclicity.

Acknowledgements

This work was made possible by the Dalhousie University Basin and Reservoir Laboratory. I would like to thank Mick O'Neill (core supervisor) at the Nova Scotia Department of Natural Resources Core Library for retrieving the core from warehouse storage and accommodating me over several days.

References

Boersma, J. 1969. Internal structure of some tidal mega-ripples on a shoal in the Westerschelde estuary, the Netherlands: report of a preliminary investigation. Netherlands Journal of Geosciences/Geologie en Mijnbouw.

Boersma, J., and Terwindt, J. 1981. Neap–spring tide sequences of intertidal shoal deposits in a mesotidal estuary. Sedimentology, **28**: 151-170.

Davies, S., Gibling, M., Rygel, M.C., Calder, J.H., and Skilliter, D. 2005. The Pennsylvanian Joggins Formation of Nova Scotia: sedimentological log and stratigraphic framework of the historic fossil cliffs.

De Boer, P.L., Oost, A., and Visser, M. 1989. The diurnal inequality of the tide as a parameter for recognizing tidal influences. Journal of Sedimentary Research, **59**: 912-921.

Friedman, G.M., and Chakraborty, C. 2006. Interpretation of tidal bundles: two reasons for a paradigm shift. Carbonates and Evaporites, **21**: 170.

Gastaldo, R.A., Bamford, M., Calder, J., DiMichele, W.A., Iannuzzi, R., Jasper, A., Kerp, H., McLoughlin, S., Opluštil, S., and Pfefferkorn, H.W. 2020. The Coal Farms of the Late Paleozoic. *In* Nature through Time. Springer. pp. 317-343.

Gibling, M., Culshaw, N., Pascucci, V., Waldron, J., and Rygel, M. 2019. The Maritimes Basin of Atlantic Canada: Basin Creation and Destruction During the Paleozoic Assembly of Pangea. *In* The Sedimentary Basins of the United States and Canada. Elsevier. pp. 267-314.

Gibling, M.R., Culshaw, N., Rygel, M.C., and Pascucci, V. 2008. The Maritimes Basin of Atlantic Canada: basin creation and destruction in the collisional zone of Pangea. Sedimentary basins of the world, **5**: 211-244.

Hovikoski, J., Räsänen, M., Gingras, M., Roddaz, M., Brusset, S., Hermoza, W., Pittman, L.R., and Lertola, K. 2005. Miocene semidiurnal tidal rhythmites in Madre de Dios, Peru. Geology, **33**: 177-180.

Martino, R.L., and Sanderson, D.D. 1993. Fourier and autocorrelation analysis of estuarine tidal rhythmites, lower Breathitt Formation (Pennsylvanian), eastern Kentucky, USA. Journal of Sedimentary Research, **63**: 105-119.

O'Connell, B., Dorsey, R.J., and Humphreys, E.D. 2017. Tidal rhythmites in the southern Bouse Formation as evidence for post-Miocene uplift of the lower Colorado River corridor. Geology, **45**: 99-102.

Shukla, T., and Shukla, U. 2013. Tidal bundles: An evidence of mixed tidal regime in scarp sandstone formation of the proterozoic Kaimur Group, Vindhyan Basin, Mirzapur District, (Uttar Pradesh), India. Gondwana Geological Magazine, **28**: 93-99.

Tessier, B., and Gigot, P. 1989. A vertical record of different tidal cyclicities: an example from the Miocene Marine Molasse of Digne (Haute Provence, France). Sedimentology, **36**: 767-776.

Visser, M. 1980. Neap-spring cycles reflected in Holocene subtidal large-scale bedform deposits: a preliminary note. Geology, **8**: 543-546.